

https://doi.org/10.1070/QEL17548

Emission of xenon in the spectral range of 120–800 nm upon excitation by diffuse and spark discharges

A.N. Panchenko, D.V. Beloplotov, V.V. Kozhevnikov, M.I. Lomaev, D.A. Sorokin, V.F. Tarasenko

Abstract. **Xenon emission in the spectral range of 120–800 nm upon excitation by subnanosecond voltage pulses is investigated. Excitation is performed using diffuse and spark discharges in an inhomogeneous electric field at a xenon pressure ranging from 0.3 to 3 atm. It is shown that xenon excitation by a series of successive 0.7-ns voltage pulses with a pause of 30 ns leads to a decrease in the second-continuum radiation intensity by the second and subsequent voltage pulses and an increase in the first-pulse afterglow intensity. It is confirmed that in the case of a pulsed diffuse discharge, the second continuum of xenon dimers, which is used to generate laser and spontaneous radiation in the VUV spectral region, makes the largest contribution to the radiation energy. Broadband radiation in the visible range ($\lambda > 400$ nm) is found to occur when the discharge is constricted. The obtained results indicate that the influence of the dynamic displacement current on the pin-diode caused a measurement error in the papers by V.I. Baryshnikov et al., who did not record the second-continuum radiation from xenon excited by a short homogeneous discharge.**

Keywords: *xenon emission, second continuum, VUV range, diffuse and spark discharges.*

1. Introduction

The second-continuum radiation from xenon dimers is widely used to design lasing [1–3] and spontaneous-emission [4–6] sources with a wavelength of 172 nm. Different regimes of homogeneous discharges [4–8] and electron beams [1–3, 9] are applied for excitation. High-power emission of xenon, krypton, and argon dimers was detected in pulsed diffuse discharges initiated by runaway electrons in an inhomogeneous electric field [6, 7, 10]. In particular, emission pulses peaking at a wavelength of 172 nm, with an FWHM of 8 ns and full-angle power of ~1 MW at a discharge volume in Xe of about 1 cm^3 and a pressure of 12 atm, were obtained in [6]. At the same time, when exciting xenon in a spark discharge, recombination radiation was found to make the main contribution to the spectrum [11]. Note also that the Planck radiation of equilibrium plasma is recorded from the discharge region in xenon at large specific power inputs (spark and arc combustion regimes) [12–14].

A.N. Panchenko, D.V. Beloplotov, V.V. Kozhevnikov, M.I. Lomaev, D.A. Sorokin, V.F. Tarasenko Institute of High Current Electronics, Siberian Branch, Russian Academy of Sciences, prosp. Akademicheskii 2/3, 634055 Tomsk, Russia; e-mail: alexei@loi.hcei.tsc.ru

Received 2 March 2021; revision received 8 April 2021
Kvantovaya Elektronika **51** (7) 649–654 (2021)
Translated by Yu.P. Sin'kov

The amplitude–time and spectral characteristics of xenon radiation that were reported in recent studies [15, 16] differ radically from the previous data on xenon excitation in a diffuse discharge with a nanosecond voltage pulse [5–7, 10]. It was stated in [16] that '…the emission spectrum of a high-voltage discharge of sub-nanosecond duration with a hemispherical cathode in the regime of a volume discharge in xenon has a continuum shape and can be approximated in the measured wavelength range of 110–400 nm by the Planck distribution with a maximum at 30 nm. The radiation power at a storage energy of about 0.3 J was 12 MW and the duration of the radiation pulse did not exceed 1 ns. The characteristics of the spectrum virtually do not change with a change in the working gas pressure in the range 0.1–3 atm'.

The development of a compact 12-MW radiation source with a spectral distribution peaking at $\lambda = 30$ nm and excitation pulse energy as low as 0.3 J is very promising for different applications. However, it is unclear why the authors of [15, 16] did not record the emission of xenon dimers, which was observed in the homogeneous plasma formed by electron beams or discharges in all publications known to us (see, for example, [2–4] and references therein). We also revealed a strong second-continuum band of xenon dimers in the spectrum of xenon excited by nanosecond voltage pulses [5–7, 10].

The second specific feature of the results reported in [15, 16] is that the Planck radiation was observed in a uniform discharge at a smaller specific power input in comparison with the power input in the discharge channel stage. As can be understood from [16], a discharge with channels was formed with an increase in the capacitance of pulsed oscillator capacitors. It is known that a spark discharge in xenon generates high-power recombination or Planck radiation in the visible and UV spectral regions (see, e.g., [11–14]), and emission of xenon dimers is observed in a uniform discharge [4–8, 10].

In addition, it is not quite clear why the amplitude of the signal from a fast pin-diode FDUK-1UVSKM remained almost constant with a change in the xenon pressure by more than an order of magnitude in the aforementioned studies (see identical plots in Fig. 3 in [15] and Fig. 5 in [16]). It is well known that the intensity of radiation from Xe_2^* dimers in a homogeneous plasma, formed in xenon by both electron beams and discharges, increases with increasing pressure in the range of 0.3–3 atm.

In this paper, we report the results of a comprehensive study of the emission characteristics of diffuse and constricted discharges in xenon in the pressure range of 0.3–3 atm, formed by a 0.7-ns voltage pulse, and compare these results with the data of [15, 16].

2. Experimental

We investigated the emission and current–voltage characteristics of discharge in a chamber schematically shown in Fig. 1. The chamber had two CaF_2 windows, before which a vacuum monochromator, a spectrometer, and an FEK-22SPU photocell or a camera were installed. The best way to form a diffuse discharge at small interelectrode gaps with the maximum delay to the instant of spark formation is to use both electrodes with a small curvature radius. It was established previously [17] that the polarity of voltage pulses did not affect significantly the diffuse discharge formation and that the negative polarity of a small-curvature electrode made it possible to detect easily the runaway electron beam [10, 18]. Therefore, both electrodes used by us were made of segments of 5.6-mm-long sewing needles with a base diameter of 0.75 mm and a rounding tip radius of 40 μm. One electrode was fixed to a cone, which passed into a cylinder 6 mm in diameter, and the second electrode was fixed to a flat grounded flange. Using two needle electrodes with a small distance between them, we could reduce the excited volume for both diffuse and constricted discharges, and, correspondingly, increase the specific energy input.

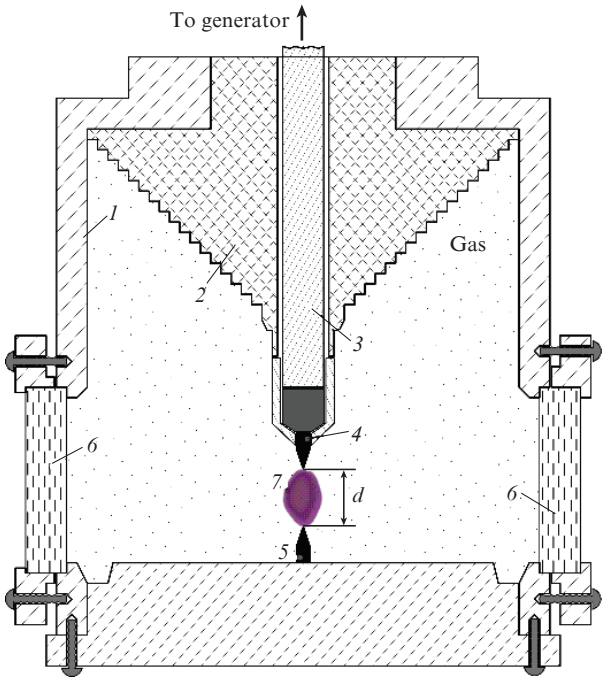

Figure 1. Discharge chamber design:
(*1*) chamber housing; (*2*) insulator; (*3*) high-voltage input; (*4*, *5*) needle-shaped cathode and anode; (*6*) CaF_2 window; (*7*) discharge region; $d = 4$ mm is the interelectrode gap.

The discharge glow was photographed by a digital camera. The emission spectra were recorded in the range from 200 to 800 nm using an EPP2000C-25 spectrometer (StellarNet-Inc.) with a known spectral sensitivity; in the range of 120–540 nm we applied a VM-502 vacuum monochromator (Acton Researcher Corp.). The time characteristics of emission in some spectral ranges were measured using an EMI 9781 B photoelectron multiplier, which made it possible to resolve the leading edge of signal with a duration of ~3 ns and the trailing edge ~30 ns long, and an FEK-22SPU photodiode with a time resolution of ~1 ns. Optical signals and voltage pulses were recorded using a TDS-3034 oscilloscope with a bandwidth of 0.3 GHz (2.5 G s^{-1}). Voltage pulses were also recorded by a digital oscilloscope KeySight MSOS804A (6 GHz, 20 G s^{-1}).

We applied a voltage pulse generator GIN-55-01 [19], which formed pulses of negative polarity with an amplitude in the incident wave up to 38 kV and FWHM $\tau_{0.5} \approx 0.7$ ns at the leading edge duration $\tau_{0.1-0.9} \approx 0.7$ ns. As a result, the voltage amplitude across the discharge gap in the absence of breakdown could reach 76 kV. Voltage pulses were applied to electrodes through a 3-m-long cable with a wave resistance of 75 Ω and recorded by a capacitance divider, which was mounted near the discharge gap or at a distance of 1 m from it. Figure 2 shows the voltage waves (one incident on the discharge gap and the other reflected from it) in the open-circuit mode.

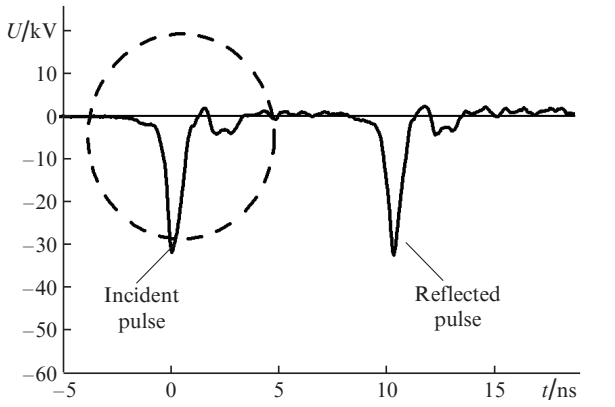

Figure 2. Oscillograms of the incident and reflected voltage waves under open-circuit conditions. The distance from the capacitance divider to the chamber is 1 m, and the voltage pulse amplitude at the generator output is 32 kV.

The application of voltage pulses to a discharge gap through a cable 3 m long allowed us to record the emission from a discharge induced by a voltage pulse with an FWHM of 0.7 ns during the first 30 ns. Then reflected pulses arrived at the gap. The interelectrode gap was varied from 1 to 10 mm in preliminary experiments. An increase in the gap width led to an increase in the delay time of breakdown, which could be observed not in the first pulse. In the case of narrow gap a diffuse discharge arose at the leading edge of the voltage pulse, and the time preceding its constriction decreased.

At wide gaps discharge constriction was absent. The data reported below were obtained at an interelectrode gap $d =$ 4 mm and a pulse repetition frequency of 10 Hz. A transformation of diffuse discharge into the spark mode was observed during arrival of reflected pulses.

3. Results

At a gap width $d = 4$ mm and xenon pressure of 0.3–3 atm, a breakdown was observed at an incident wave voltage of 32 kV with a delay of no more than ~1 ns. Figure 3 shows the voltage pulses recorded by a capacitance divider mounted at a distance of 9.5 cm from the discharge gap. When a breakdown occurred, the resistance of xenon plasma discharge became much lower than the cable wave resistance for several

tenths of a nanosecond. Therefore, the part of the voltage pulse preceding the breakdown (in the open-circuit mode) was reflected from the discharge gap with the same polarity and amplitude, whereas the pulse part after the breakdown was reflected with opposite polarity. The wave resistance of the generator after the formation of voltage pulse becomes much lower than the cable resistance for less than 15 ns. Correspondingly, the voltage pulses and their parts were reflected from the generator with opposite polarity. As a result, the first part of the pulse (prior to the breakdown) arrived at the gap with a change in polarity, whereas the second part, due to the fast breakdown and drop of the gap and generator resistances to small values, arrived without a change in polarity. Therefore, the main part of the second pulse had the same polarity as the first pulse.

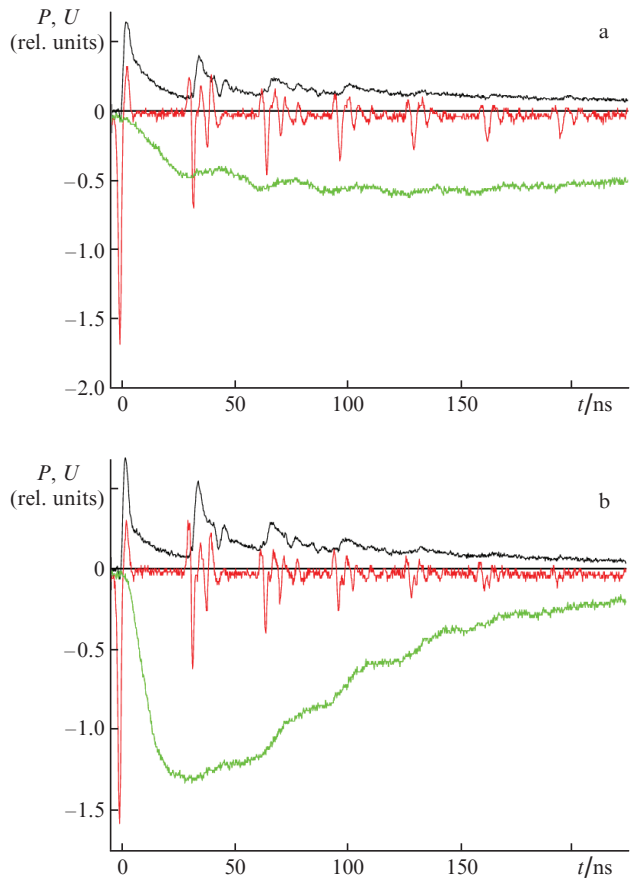

Figure 3. (Colour online) Synchronised oscillograms of voltage pulses (U, red lines) and powers of xenon dimer radiation at λ = 172 nm (P, green line) and the radiation recorded by FEK-22 in the wavelength range of 200–600 nm (P, black lines). Xenon pressure is (a) 0.6 and (b) 1.8 atm.

The positive spike in Fig. 3 is pronounced for the second pulse. In addition, negative pulses can be seen well for subsequent reflections. The number of reflected pulses and their amplitudes depended on the resistance of xenon plasma in the gap. The plasma resistance increased with increasing pressure, while the number of reflected pulses decreased. The influence of the generator resistance was weak, and the cable losses were small. At a gap resistance equal to the cable wave resistance, we recorded only one pulse with an FWHM of 0.7 ns.

The setup in use made it possible to observe for the first 30 ns the emission from xenon excited by a single voltage pulse with an FWHM of 0.7 ns. The voltage pulses used in [15, 16] were hardly shorter, as follows from the schematic of the setup reported in [16], where pulses were generated by a voltage pulse generator with two dischargers.

The existence of several excitation pulses with a 30-ns interval between them, which is due to the presence of a cable between the generator and discharge chamber, provided additional information about the xenon emission characteristics. For example, as can be seen in Fig. 3, the xenon emission power begins to grow after the arrival of reflected pulses, which can be explained by the additional power input from them. The power of discharge radiation in the visible and UV spectral regions behaves similarly.

As investigations showed, at given values of voltage pulse duration and the interelectrode gap, the second continuum of radiation from Xe_2^* dimers, peaking at λ = 172 nm, in the emission spectrum of discharge in xenon at pressures of 0.3–1 atm always had the highest spectral energy density Q in the range of 120–520 nm (Fig. 4).

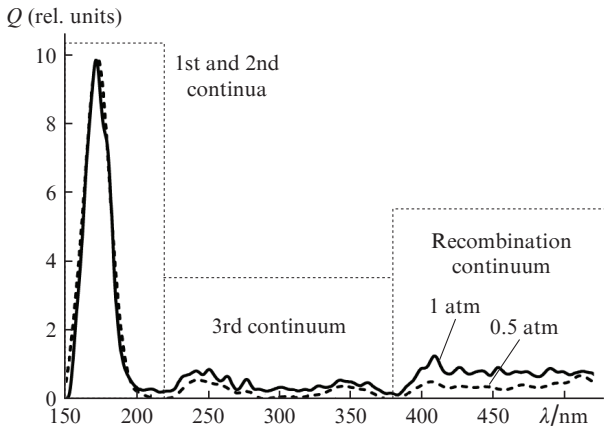

Figure 4. Xenon radiation at pressures of 0.5 and 1 atm.

The dominance of the second-continuum radiation from xenon dimers indicates the occurrence of a diffuse discharge in the gap during the first voltage pulse. The reported spectrum in the range of 200–400 nm exhibits radiation of the third continuum, which consists of two bands and is observed with excitation in different ways [7], as well as the wide band in the wavelength range above 400 nm. The latter band can be assigned to recombination radiation from xenon, which occurs in spark discharges [11]. With an increase in xenon pressure the second-continuum power increases, while the FWHM decreases (see Fig. 3). Therefore, the radiation energy of xenon dimers at pressures of 0.5 and 1 atm remains constant in Fig. 4. The spectral energy densities of the third-continuum radiation and recombination radiation increase with an increase in xenon pressure.

Note that the peak in the distribution of the spectral energy density of the second-continuum radiation from xenon dimers is observed at λ = 172 nm; this radiation dominates in the range of 150–520 nm. Second continua were recorded in these experiments in the entire pressure range under study, as well as and the third continua of xenon in the range of 250–400 nm. The intensity of the wide band due to the recombination radiation in the wavelength range above 400 nm

increased with an increase in pressure, which can be explained by the higher rate of transformation of diffuse discharge into the spark mode.

The integral photograph of the discharge gap and xenon emission spectra from different discharge regions are presented in Fig. 5. At a pressure of 1 atm one can see the region of diffuse discharge about 2.5 mm in diameter at the cathode and brighter radiation of the spark channel, whose intensity is higher near the electrodes. The bright channel diameter was about 0.7 mm under these conditions. As can be seen in Fig. 5b, the intensities of continuum glow, peaking at wavelengths near 500 nm, and individual lines of xenon and electrode material from the plasma increase significantly near the needle electrodes.

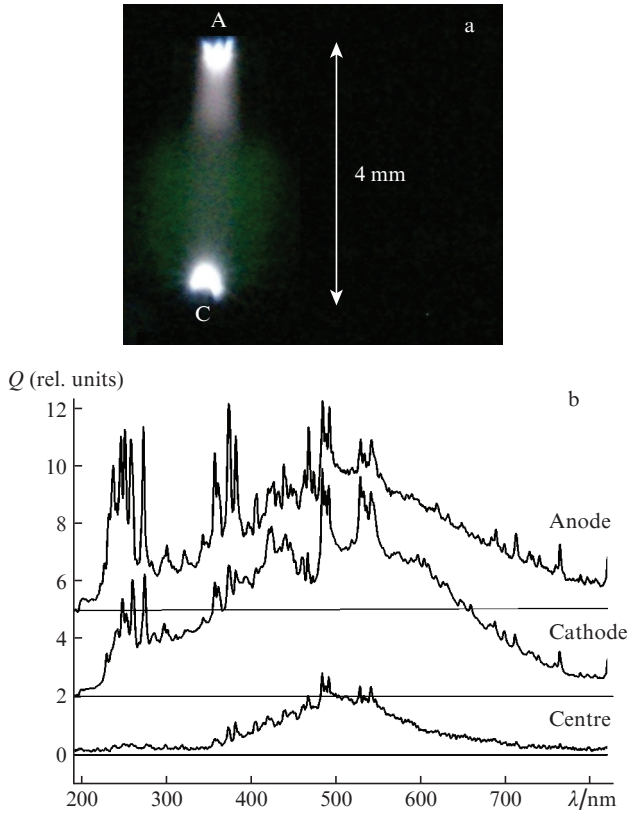

Figure 5. (a) Integral photograph of discharge in Xe and (b) emission spectra from the centre of discharge gap and near-electrode regions at a xenon pressure of 1 atm.

The data reported above are in good agreement with our previous results, obtained for a discharge initiated by voltage pulses with an amplitude of 220 kV and FWHM (in the matched regime) of 2 ns, produced by a RADAN-220 generator [6, 7]. With an increase in pressure the amplitude of second-continuum radiation pulses from xenon dimers increased, whereas the pulse duration decreased.

The radiation in the range of 200–520 nm has two main components (see Figs 3, 4). The first one, with a short de-excitation time, can be assigned to the radiation of the third continua of xenon in the range of 200–400 nm [7]. The second component is the recombination radiation from the constricted discharge [11]. The arrival of reflected voltage pulses at the discharge gap leads to an increase in the intensity of the third-continuum and recombination radiation; however, it does not affect much the second-continuum intensity (see Fig. 3).

4. Analysis of the main results of [15, 16]

It was stated in [15, 16] that the spectral distribution of radiation from plasma of a high-voltage subnanosecond bulk discharge in Xe at pressures of 0.1–3 atm can be approximated by the Planck distribution peaking at $\lambda = 30$ nm. The pulse duration and power input to the discharge plasma did not exceed 1 ns and 0.3 J, respectively. However, estimates show that this power input is insufficient to heat the amount of xenon taken in [16] to the aforementioned temperature of 1.1×10^5 (in order to excite it). The estimation was based on the well-known relation [20]

$$q = CM(T_2 - T_1), \tag{1}$$

where q is the amount of heat; C is the specific heat; M is the gas mass; and T_2 and T_1 are the final and initial temperatures, respectively. According to [21], the specific heat upon isochoric xenon heating (the voltage pulse duration was indicated to be 0.2 ns in [16]) is $\sim$18.8 J mol^{-1} K^{-1}. The xenon amount in moles was estimated proceeding from the pressure and excited volume of xenon (0.5–1 cm^3) in [16] (Fig. 6).

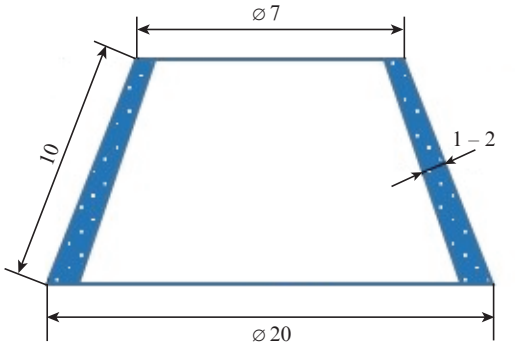

Figure 6. Estimated sizes (in mm) of the region excited by pulsed discharge in the bulk combustion regime in [16].

At a xenon pressure of 1 atm, the energy required to heat the aforementioned amount of xenon to a temperature of 1.1×10^5 K ranges from 46 to 92 J, that is, it exceeds significantly the energy stored by the generator. In addition, as was noted in [14], the characteristic plasma temperatures in high-power gas-discharge sources of spontaneous radiation do not exceed $\sim$4 eV. A further increase in plasma temperature upon ohmic heating in open discharges, without any limitation of the thermal expansion of discharge region is inefficient because of a decrease in the energy transfer rate from electrons to ions. We consider also as debated the results of [16] that concern, first, the absence of influence of xenon pressure in the range of 0.1–3 atm on the plasma radiation intensity (Fig. 5 in [16]) and, second, the duration of the radiation pulse from discharge plasma in the bulk combustion regime below 1 ns. It is known well that a variation in pressure leads to a change in the plasma resistance, which changes the energy input into the discharge plasma and, correspondingly, the radiation intensity. The characteristic radiation pulse duration for an equilibrium plasma (heated initially to a temperature T_{max}) upon cooling can be estimated based on the Stefan–Boltzmann

law: $R = \sigma T^4$, where R is the energy brightness, T is the temperature of absolutely black body, and σ is the Stefan – Boltzmann constant. Let us estimate the characteristic duration of a plasma radiation pulse taking into account only the radiative losses:

$$dq = mc dT = -S\sigma T^4 dt, \quad (2)$$

where dq is the plasma energy losses for a time dt; m and c are, respectively, the mass and specific heat of excited gas; and S is the plasma region surface area. The solution to differential Eqn (2) with respect to the radiation power $P(t) = S\sigma T^4$ has the form

$$P(t) = \sigma S\left(\frac{3\sigma S t}{mc} + \frac{1}{T_{\max}^3}\right)^{-3/4}. \quad (3)$$

The plot of the function $P(t)$ for the conditions considered in [16] is shown in Fig. 7. It can be seen that, upon instantaneous heating, the pulse FWHM is ~7 ns, which exceeds significantly the pulse duration reported in [16]. In addition, a noteworthy feature is the inconsistency between the shapes of pulse trailing edges in the experiment performed in [16] and in Fig. 7. It follows from all the aforesaid that the suggestion made in [15, 16] about the heating of xenon plasma to a temperature of 1.1×10^5 K and the reported corresponding radiation characteristics are not confirmed by simple estimates of plasma parameters for the experimental conditions used in [15, 16].

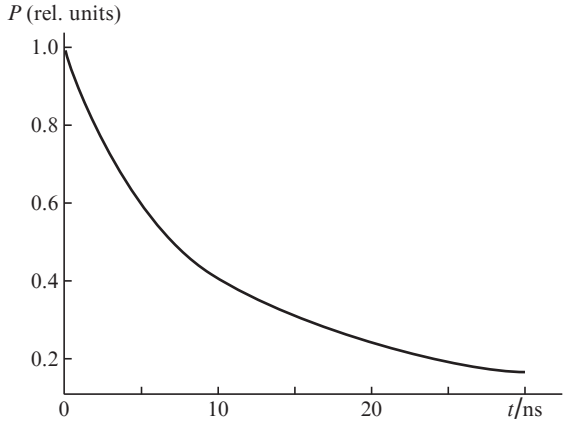

Figure 7. Time dependence of radiation power P, calculated according to (3).

There are also no specific data in [15, 16] on the values of the discharge voltage and current, as well as on the durations and shapes of voltage and current pulses under the 'volume- and streamer-discharge' conditions. It was only said that 'The design of the capacitors (C1 and C2) of the Marx generator makes it possible to change their capacitance, which provides the control of the duration of the discharge pulse'. Apparently, the 'streamer-discharge' regime in [16] corresponded to a spark discharge. Under these conditions, relatively long emission pulses were observed in the visible and near-UV regions (see Fig. 4 in [16]). These data coincide mainly with our results of studying constricted discharges in xenon [6, 7].

As was shown in this study, the second-continuum radiation from xenon dimers in the range of 150–520 nm dominates under diffuse-discharge conditions. The duration of the radiation pulse exceeds significantly the excitation pulse duration and, as well as its amplitude, depends on the gas pressure. Figure 3 in [16] shows a radiation pulse (signal from a pin-diode, with the window open to the discharge chamber) having an FWHM of ~1 ns at a xenon pressure of 0.3 atm. The dependences of pin-diode pulse amplitudes for the UV and VUV spectral regions are presented in Fig. 5 in [16]. These data indicate that the radiation power depends weakly on xenon pressure, and its amplitude increases significantly at an open window of the pin-diode. However, the emission spectra for a volume discharge in the wavelength range of 30–200 nm were not reported in [15, 16].

We believe that the small variation in the pin-diode signal amplitude with a change in xenon pressure, as well as the small duration of the emission pulse in the VUV spectral region, indicate that the measurements performed in [15, 16] were erroneous. It is known that, when a high-voltage pulse with a subnanosecond leading edge is applied at the discharge gap, the collector [22] and photodetector [23] can record (through a grid anode) the dynamic displacement current (DDC) [24], which arises when the capacitor formed by the plasma front and receiving electrode of collector or photodetector is charged. At high overvoltages the duration of DDC pulse may amount to several hundred picoseconds, and its amplitude may reach several (or even several ten) amperes [24]. Apparently, the authors of [15, 16] disregarded the influence of DDC on the pin-diode.

The absence of high-power signals from the pin-diode under the 'streamer' discharge conditions is due to the increase in the duration of the voltage pulse leading edge with an increase in the capacitance of generator capacitors and the corresponding decrease in the breakdown voltage. The rise in the radiation intensity with a decrease in wavelength in Fig. 4 in [16] can be explained by the contribution of the edge of the second-continuum emission band of xenon dimers, whose intensity exceeds significantly that of constricted discharge radiation in other spectral regions, as well as the third-continuum radiation from xenon.

5. Conclusions

The study of the emission of xenon excited by voltage pulses with a 0.7-ns FWHM revealed that the second-continuum radiation from Xe_2^* dimers dominates in the spectrum of the diffuse discharge in xenon. In the pressure range of 0.3–3 atm its intensity increases, while the FWHM decreases. This circumstance makes it possible to design lasers based on xenon dimers with diffuse-discharge excitation [25] using extended electrodes shaped as razors. The third-continuum radiation from xenon with a short pulse duration was detected in the range of 200–400 nm. Additional excitation of xenon plasma by a series of voltage pulses reflected from the discharge gap and generator may lead to discharge constriction and occurrence of broadband recombination radiation, against the background of which xenon ion lines can be seen. Discharge constriction begins near the electrodes due to the explosive electron emission [26]. Note that, using extended electrodes with a small curvature radius (e.g., in the form of razors), one can initiate a diffuse discharge in different gases and obtain efficient generation in different spectral regions, including the VUV range [25, 27].

It follows also from the obtained emission spectrum and analysis performed that, in the case of subnanosecond excita-

tion pulses and sufficiently wide discharge gaps, the Planck radiation does not make any significant contribution to the recorded radiation from xenon. We suppose that in the measurements performed in [15, 16] the pin-diode recorded a dynamic displacement current [22–24], that is, a short-term signal, which, as well as the amplitude, depended weakly on the xenon pressure.

Acknowledgements. This work was performed within a State Assignment for the Institute of High-Current Electronics, Siberian Branch, Russian Academy of Sciences (Project No. FWRM-2021-0014).

References

1. Basov N.G., Danilychev V.A., Popov Yu.M., Khodkevich D.D. *JETP Lett.*, **12**, 329 (1970) [*Pis'ma Zh. Eksp. Tekh. Fiz.*, **12**, 473 (1970)]; http://www.jetpletters.ac.ru/cgi-bin/articles/download.cgi/1735/article_26361.pdf.
2. Koehler H.A., Ferderber L.J., Redhead D.L., Ebert P.J. *Appl. Phys. Lett.*, **21**, 198 (1972); https://doi.org/10.1063/1.1654342.
3. *Excimer Lasers*. Ed. by C.K. Rhodes (Berlin, Heidelberg: Springer-Verlag, 1979); DOI: 10.1007/978-3-662-11716-3.
4. Boyd I.W., Zhang J.-Y., Kogelschatz U., in *Book Photo-Excited processes, Diagnostics and Applications*. Ed. by A. Peled (The Netherlands: Kluwer Academic Publishers, 2003) pp 161–199.
5. Lomaev M.I., Sosnin E.A., Tarasenko V.F., Shitts D.V., Skakun V.S., Erofeev M.V., Lisenko A.A. *Instrum. Exp. Tech.*, **49**, 595 (2006) [*Prib. Tekh. Eksp.*, **5**, 5 (2006)]; https://doi.org/10.1134/S0020441206050010.
6. Lomaev M.I., Mesyats G.A., Rybka D.V., Tarasenko V.F., Baksht E.Kh. *Quantum Electron.*, **37**, 595 (2007) [*Kvantovaya Elektron.*, **37**, 595 (2007)]; http://dx.doi.org/10.1070/QE2007v037n06ABEH013528.
7. Baksht E.Kh., Lomaev M.I., Rybka D.V., Tarasenko V.F. *Quantum Electron.*, **36**, 576 (2006) [*Kvantovaya Elektron.*, **36**, 576 (2006)]; http://dx.doi.org/10.1070/QE2006v036n06ABEH013232.
8. Gerasimov G.N., Krylov B.E., Loginov A.V., Shchukin S.A. *Sov. Phys. Usp.*, **35**, 400 (1992) [*Usp. Fiz. Nauk*, **162**, 123 (1992)]; http://doi.org/10.1070/PU1992v035n05ABEH002237.
9. Alekseev S.V., Ivanov N.G., Losev V.F., Mesyats G.A., Mikheev L.D., Ratakhin N.A., Panchenko Yu.N. *Quantum Electron.*, **49**, 901 (2019) [*Kvantovaya Elektron.*, **49**, 901 (2019)]; http://dx.doi.org/10.1070/QEL17050.
10. Baksht E.H., Burachenko A.G., Kostyrya I.D., Lomaev M.I., Rybka D.V., Shulepov M.A., Tarasenko V.F. *J. Phys. D: Appl. Phys.*, **42**, 9 (2009); https://doi.org/10.1088/0022-3727/42/18/185201.
11. Baksht E.Kh., Boichenko A.M., Galakhov I.V., Zolotovskii V.I., Lomaev M.I., Osin V.A., Rybka D.V., Tarasenko V.F., Tkachev A.N., Yakovlenko S.I. *Laser Phys.*, **17**, 782 (2007); https://doi.org/10.1134/S1054660X0706002397.
12. Marshak I.S., Doinikov A.S., Zhil'tsov V.P., Kirsanov V.P., Rovinskii R.E., Shchukin L.I., Feigenbaum M.G. *Impul'snye istochniki sveta* (Pulsed Light Sources) (Moscow: Energiya, 1978)
13. Kamrukov A.S., Kozlov N.P., Kuznetsov S.G., Protasov Yu.S. *Sov. J. Quantum Electron.*, **12**, 910 (1982) [*Kvantovaya Elektron.*, **9**, 1429 (1982)]; http://dx.doi.org/10.1070/QE1982v012n07ABEH005448.
14. Fortov V.E. (Ed.) *Entsiklopediya nizkotemperaturnoi plazmy* (Encyclopedia of Low-Temperature Plasma) (Moscow: Nauka, MAIK 'Nauka/Interperiodika', 2000) Vol. IV, pp 231–262.
15. Baryshnikov V.I., Chirkov V.Y., Paperny V.L. *J. Phys.: Conf. Series*, **1393**, 4 (2019); DOI: 10.1088/1742-6596/1393/1/012037.
16. Baryshnikov V.I., Paperny V.L., Chernykh A.A., in *7th Intern. Congr. Energy Fluxes Radiation Effects* (EFRE) (Tomsk, Russia, 2020) pp 107–110; DOI: 10.1109/EFRE47760.2020.9241968.
17. Shao Tao, Tarasenko Victor F., Zhang Chen, Baksht Evgeni Kh., Zhang Dongdong, Erofeev Mikhail V., Ren Chenguan, Shut'ko Yuliya V., Yan Ping. *J. Appl. Phys.*, **113**, 10 (2013); https://doi.org/10.1063/1.4794031.
18. Tarasenko V.F. *Plasma Sources Sci. Technol.*, **29**, 21 (2020); DOI:10.1088/1361-6595/ab5c57.
19. Efanov V.M., Efanov M.V., Komashko A.V., Kriklenko A.V., Yarin P.M., Zazoulin S.V., in *Ultra-Wideband, Short Pulse Electromagnetics 9* (New York: Springer, 2010) pp 301–305; DOI https://doi.org/10.1007/978-0-387-77845-7.
20. Dubrovskii I.M., Egorov B.V., Ryaboshapka K.P. *Spravochnik po fizike* (Handbook of Physics) (Kiev: Naukova Dumka, 1986).
21. Grigoriev I.S., Meilikhov E.Z. (Eds) *Handbook of Physical Quantities* (Boca Raton: CRC Press, 1997; Moscow: Energoatomizdat, 1991).
22. Beloplotov D.V., Lomaev M.I., Sorokin D.A., Tarasenko V.F. *Phys. Plasmas*, **25**, 7 (2018); https://doi.org/10.1063/1.5046566.
23. Tarasenko V.F., Baksht E.K., Burachenko A.G., Beloplotov D.V., Kozyrev A.V. *IEEE Transact. Plasma Sci.*, **45**, 76 (2016); DOI:10.1109/TPS.2016.2637570.
24. Shao T., Tarasenko V.F., Zhang C., Burachenko A.G., Rybka D.V., Kostyrya I.D., Lomaev M.I., Baksht E.Kh., Yan P. *Rev. Sci. Instrum.*, **84**, 7 (2013); https://doi.org/10.1063/1.4807154.
25. Panchenko A.N., Sorokin D.A., Tarasenko V.F. *Progr. Quantum Electron.*, **76**, 36 (2021); DOI: 10.1016/j.pquantelec. 2020.100314.
26. Korolev Yu.D., Mesyats G.A. *Avtoemissionnye i vzryvnye protsessy v gazovom razryade* (Field-Emission and Explosive Processes in Gas Discharges) (Novosibirsk: Nauka, 1982).
27. Tarasenko V.F., Panchenko A.N., Kozhevnikov V.V. *Quantum Electron.*, **50**, 900 (2020) [*Kvantovaya Elektron.*, **50**, 900 (2020)]; http://dx.doi.org/10.1070/QEL17384.